Vacuum 152 (2018) 193–199

Contents lists available at ScienceDirect

Vacuum

journal homepage: www.elsevier.com/locate/vacuum

Effect of nitrogen ion irradiation parameters on properties of nitrogen-containing carbon coatings prepared by pulsed vacuum arc deposition method

A.I. Poplavsky [a], A. Ya. Kolpakov [a], Yu. Kudriavtsev [b, *], R. Asomoza [b], I. Yu. Goncharov [a], M.E. Galkina [a], S.S. Manokhin [a], V.A. Kharchenko [a]

[a] Federal State Autonomous Educational Institution of Higher Education, Belgorod National Research University, 85 Pobeda Str., Belgorod, 308015, Russia
[b] Departamento Ingeniería Eléctrica - SEES, CINVESTAV, Mexico

ARTICLE INFO

Article history:
Received 25 January 2018
Received in revised form
18 March 2018
Accepted 19 March 2018
Available online 20 March 2018

Keywords:
Ta-C
Vacuum arc deposition
Nitrogenated ta-C
Ion irradiation

ABSTRACT

Studies of the effect of nitrogen ion irradiation on the structure and properties of nitrogenated amorphous carbon coatings prepared on polished sitall and silicon substrates by the pulsed vacuum arc deposition method are presented. The techniques used in the investigations were electron energy loss spectroscopy, Raman spectroscopy, and atomic force microscopy. The elemental composition of the coatings was estimated by secondary ion mass spectrometry. It has been found that an increase in the intensity of nitrogen ion irradiation of a carbon nitrogen-containing coating results in an increase in its electrical conductivity, decreases in internal stresses, density, and modulus of elasticity, and also changes in the structure and morphology of the surface. In an additional experiment with a thin a-C:N layer the absence of nitrogen diffusion in a-C during annealing at the temperature up to 1000 °C was confirmed.

1. Introduction

Diamond-like carbon (DLC) coatings, also known as amorphous carbon (a-C), are attractive for microelectromechanical systems (MEMS) [1] and biomedicine [2]. The structure and properties of DLC coatings can be varied in wide limits by doping with nitrogen, which opens up the possibility of obtaining new functional coatings. The addition of nitrogen to an amorphous DLC coating matrix results in higher electrical conductivity [3–5] and emission characteristics [6], a more developed surface relief [4,7], lower residual stresses [4,8], and modified mechanical properties [4,9].

If DLC coatings are obtained by the vacuum arc deposition method, their doping is typically carried out by filling the vacuum chamber with the nitrogen gas, the dissociation and ionization of molecules of which occur directly in the flow of highly ionized carbon plasma [3,5,7]. The partial nitrogen pressure is varied from 10^{-7} to 10^{-2} mbar. In Refs. [4,9], the N_2 gas was fed into the chamber by using a radio-frequency ion beam source, and an ionized gas flow with ion energy of 0–1000 eV was obtained at the output. The incident angle was set at 30° to the normal of the substrate. Abnormally high hardness and modulus of elasticity obtained by the nanoindentation method were observed at a nitrogen ion energy of 100 eV. When the ion energy was further increased, these properties became poorer. In Ref. [8], another approach to controlling the coating properties was used. It involved studies of the effect of a negative accelerating potential applied to the substrate on the structure and properties of the nitrogenated tetrahedral amorphous carbon (ta-C:N) thin films prepared by pulsed vacuum arc deposition. Of interest was a nitrogen content increase in the coating as the accelerating potential increased to 100 V followed by a nitrogen content decrease when the potential exceeded this value.

Analysis of the publications mentioned above shows that properties of nitrogen-containing carbon coatings depend on the method and technological parameters of fabrication and are mainly determined by the percentage ratio of the bonds formed due to the sp^1, sp^2, and sp^3 hybridizations, which in their turn depend on the ion energy and nitrogen content in the coating. Our goal was to study the effect of nitrogen ion irradiation on the structure and properties of the nitrogenated amorphous carbon (ta-C:N) coatings obtained on substrates of a dielectric sitall and semiconductor silicon by the vacuum arc deposition method without applying an

* Corresponding author.
E-mail address: yuriyk@cinvestav.mx (Yu. Kudriavtsev).

https://doi.org/10.1016/j.vacuum.2018.03.028
0042-207X/

accelerating potential. The nitrogen pressure in the vacuum chamber was kept constant, and the irradiation intensity was varying by the discharge voltage of an ion source with a closed electron drift.

2. Experimental

The schematic of the reactor for the vacuum arc deposition method of obtaining ta-C:N coatings under nitrogen ion irradiation is shown in Fig. 1. The source of the carbon plasma is a pulsed source with a graphite cathode described in Ref. [10].

A cathode (3) was made from graphite of the GS-1900 grade. Because of a pulsed vacuum arc discharge the cathode (3) was sputtered and converted into carbon plasma. The plasma was accelerated in the cathode (3) - anode (6) gap. The accelerated plasma flow was focused by a coil (7) and, by depositing on a substrate (2), formed a carbon coating. The pulsed arc was powered by a capacitor bank with a capacity of 2000 μF charged to a voltage of 300 V. The repetition rate of discharge pulses was 2 Hz.

The gas was introduced into the vacuum chamber by using a gas ion source (8), which was an ion accelerator with a cold cathode (10) and an azimuthal electron drift. At the output, the source had an annular ion beam with a diameter of about 100 mm. Sources of this type form a no monoenergetic beam, the average ion energy in the beam is 250 ± 750 eV. It is determined by the discharge voltage and gas pressure.

The substrate was arranged horizontally in such a way that the angle of incidence of ions of carbon and gas was from 30° to 45° to its surface. Owing to such an arrangement of the substrate, uniform coatings with lower internal stresses could be obtained [11,13]. The substrates used were (i) sitall CT50-1-1-0.6 for studies of the surface morphology and electrical and mechanical properties of the a-C:N coatings, and (ii) silicon n-type conductivity with the (100) orientation for determining the elemental composition, obtaining Raman spectra, and estimating internal stresses. The coating thickness was 100 ± 10 nm.

The vacuum chamber was preliminarily pumped down to a pressure of 3×10^{-3}Pa, and the substrate surface was cleaned by etching with argon ions with the help of the gas ion source (8). Then the a-C:N coatings were deposited on the substrates by the vacuum arc deposition method by feeding nitrogen (N_2) into the chamber through the gas ion source (8) to a pressure of 0.1 Pa. The discharge voltage U of the ion source was varied from 0 to 2 kV, the discharge current was 0–72 mA and the ion current density was 0–0.1 mA/cm^2. The substrate temperature was <60 °C. The coating growth rate was 0.1 nm/pulse, which was 12 nm/min at a discharge pulse frequency of 2 Hz. The etching rate of the a-C:N coatings with nitrogen ions at a discharge voltage of 2 kV was approximately 2.1 nm/min.

The elemental composition of the a-C:N coatings was determined by Secondary Ion Mass-Spectrometry, SIMS. We used a TOF-SIMS-V time-of-flight mass spectrometer from ION-TOF GMBH (Germany). The layer analysis was carried out in the two-beam mode: the surface was sputtered (300 × 300 μm) by a cesium ion beam with an energy of 2 keV, the central part of the etching crater (100 × 100 μm) was analyzed by using a pulsed source of bismuth ions with an energy of 30 keV. Negative secondary ions separated in mass in the time-of-flight mass spectrometer of the "reflectron" type were analyzed. The experimental etching craters were measured with a Bruker Dektak XT profiler with an error of 4%. Quantitative analysis was carried out by using implanted standards.

We applied SIMS also for a special study of nitrogen diffusion in undoped DLC. To do that a special DLC thin film with a delta-doped layer of a-CN-N was grown. Then the sample was annealed at 600 °C and 1000 °C during 40 min in a vacuum oven.

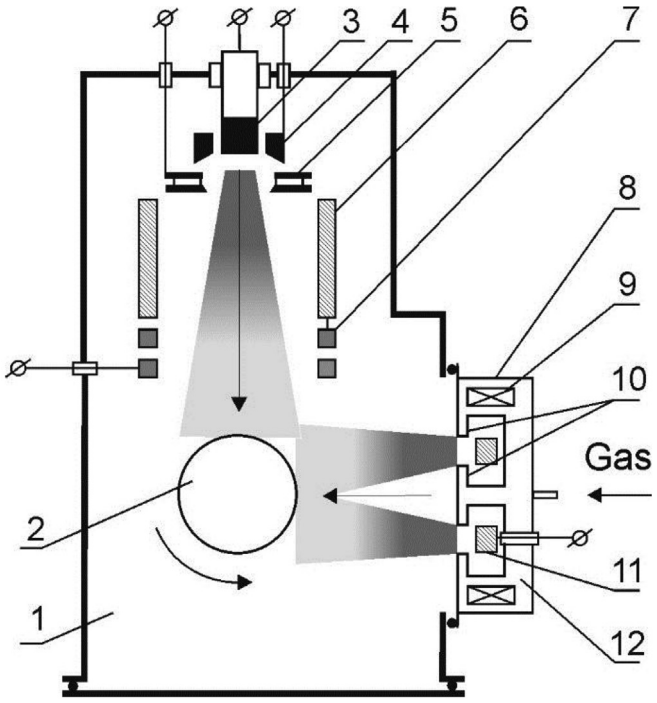

Fig. 1. Schematic of reactor for vacuum arc deposition method of preparation of ta-C:N coatings under nitrogen ion irradiation. 1 – vacuum chamber; 2 – substrate; 3 – graphite cathode; 4 – anode 1; 5 – ignition; 6 – anode 2; 7 – focusing coil; 8 – gas ion source of the "Radical" type; 9 – solenoid; 10 – cathode; 11 – anode; 12 – magnetic conductor.

To investigate the electrical conductivity of the a-C:N coatings, they were deposited on dielectric substrates of polished sitall 30 × 10 mm in size. Electrical contacts were obtained by painting with a silver conducting paste. The specific electrical conductivity of the coatings was determined from direct resistance measurements.

The morphology of the a-C:N coating surfaces was examined by a NTEGRA-AURA scanning probe microscope. The images were obtained in the contact mode of atomic-force microscopy (AFM) by using cantilevers of the CSG11 series. The scanning area was 2.5 × 2.5 μm. The electrical properties of the coating surface were investigated by the spreading resistance imaging technique. A voltage of 0.1 V was applied between the cantilever and coating, and the current distribution over the coating surface was obtained. The AFM image was processed according to ISO 25178–2:2012 by using the software package "Image Analysis P9" (NT-MDT). The software package allows calculation of S or 3D parameters which characterize the structure in the three-dimensional space.

The modulus of elasticity of the sample was estimated by AFM from the dependence of variations in the probe oscillation frequency on its base displacements [12]. To this end, the probe with an indenter in the form of a trihedral diamond Berkovich pyramid at its free end which oscillated in the direction of the normal to the sample surface with an amplitude of ~5 nm and a frequency of 10 kHz was brought into contact with the surface. As a result of interaction of the indenter with the material, the oscillation frequency of the probe changed as it the pressure on the surface. The frequency variations depended on the probe and indenter characteristics and also on elastic properties of the sample in the contact zone. The internal stresses were measured by the method described in Ref. [13].

Structural studies were carried out by a transmission electron

microscope Tecnai G2 F20 S-TWIN by Electron Energy Loss Spectroscopy (EELS). The 30-nm thick coatings were deposited on a fresh NaCl cleavage and then the coating was separated from the substrate by using a standard procedure. The coating density was calculated from the plasmon energy according to the procedure described in Ref. [14]. Raman spectra were obtained with a Renishaw in Via Basis spectrometer, the laser wavelength was 514 nm, the power was 50 mW.

3. Experimental results

According to SIMS, the a-C:N coatings obtained without an additional nitrogen ionization (U = 0 kV) contained carbon, nitrogen, oxygen, and hydrogen (Fig. 2). All the elements were distributed uniformly throughout the coating thickness. The presence of oxygen and hydrogen was due to an insufficiently deep vacuum. The total content of oxygen and hydrogen in all samples was less than 1 at.%. An increase in the discharge voltage of the ion source led to increasing intensity of dissociation and ionization of N_2 molecules and also to an increase in the energy and current density of the nitrogen ion beam which bombarded the substrate. This resulted in an increase in the nitrogen concentration in the coating and a decrease in the resistivity in a certain range (Fig. 3). The nitrogen-carbon (N/C) ratio in the a-C:N coating increased from 0.06 to 0.13 as U increased from 0 to 2 kV. The resistivity decreased from 16 to 2 Ω cm as U increased from 0 to 1 kV, then it slightly increased in the interval 1–2 kV. According to [3,4], the resistivity of ta-C coatings lies in the range 10^7–10^9 Ω cm. When nitrogen is supply into a vacuum chamber to a pressure of 0.1 Pa, a nitrogen-doped carbon coating with a resistivity of 2.5 Ω cm can be obtained on a semiconductor silicon substrate by a pulsed vacuum arc discharge [5].

Fig. 4 shows spectra of electron energy loss due to the excitation of electrons of inner shells (K-edge) of the elements of the a-C:N coating matrix. The K-edge of carbon exhibits an intense σ^* peak with a maximum at about 295 eV characteristic of carbon atoms with the sp^3 bond and a weak π^* peak (about 285 eV) indicating that there is a small number of bonds formed due to the sp^2 hybridization of electron orbitals between carbon atoms. As the discharge voltage of the ion source increases, a slight increase in the π^* peak intensity is observed in the carbon K-edge spectrum, and a significant increase in the π^* peak intensity (about 398 eV) is observed in the nitrogen K-edge spectrum with increasing nitrogen concentration. Nitrogen forms bonds with carbon by replacing carbon atoms with the sp^2 and sp^3 hybridization. As U increases from 0 to 2 kV, the number of nitrogen atoms with the sp^2 bond appreciably increases. The study of the low-energy part of the spectrum of the a-C:N coatings also revealed a decrease in the plasmon energy from 29 to 27.2 eV as U increased from 0 to 2 kV. The plasmon energy is related to the local density of valence electrons [14] and correlates with the carbon coating density. Therefore, it can be an indicator of a change in the ratio of atoms

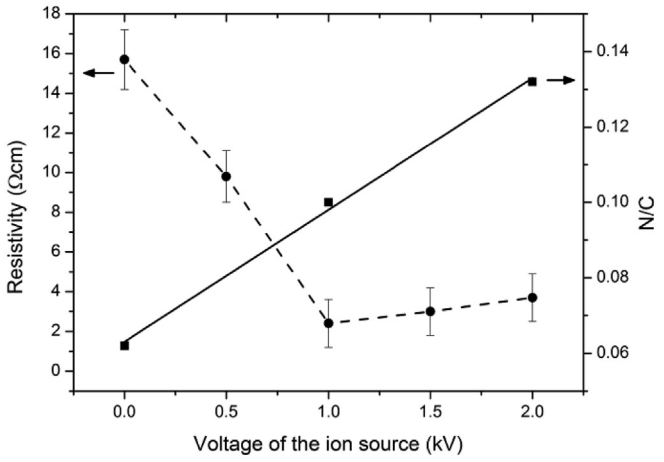

Fig. 3. Resistivity of a-C:N coating and nitrogen-carbon (N/C) ratio versus gas ion source voltage.

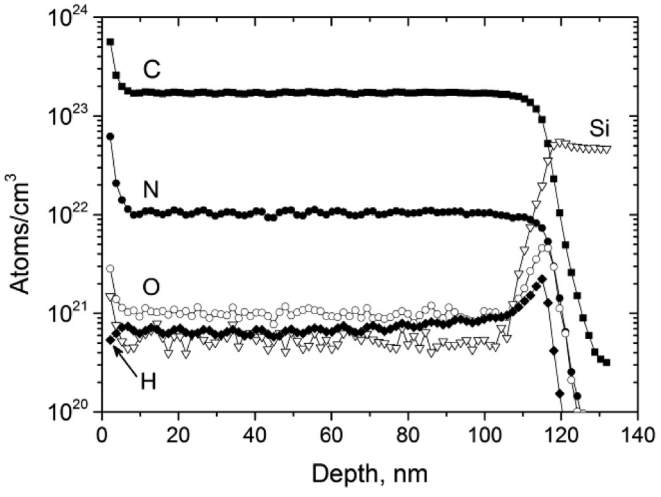

Fig. 2. Elemental composition of a-C:N coatings obtained without an additional nitrogen ionization (U = 0 kV).

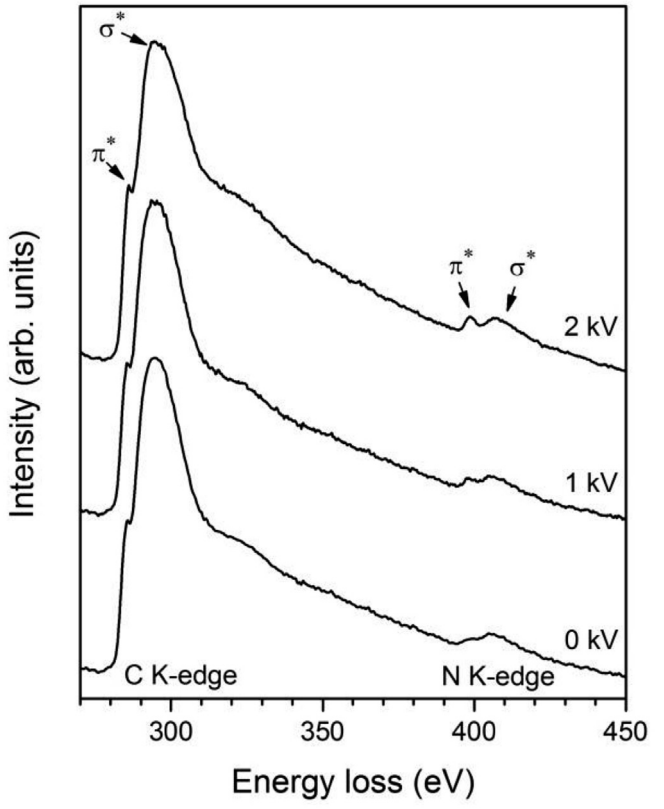

Fig. 4. EELS spectra of a-C:N coatings obtained under gas ion source voltages of 0, 1, and 2 kV.

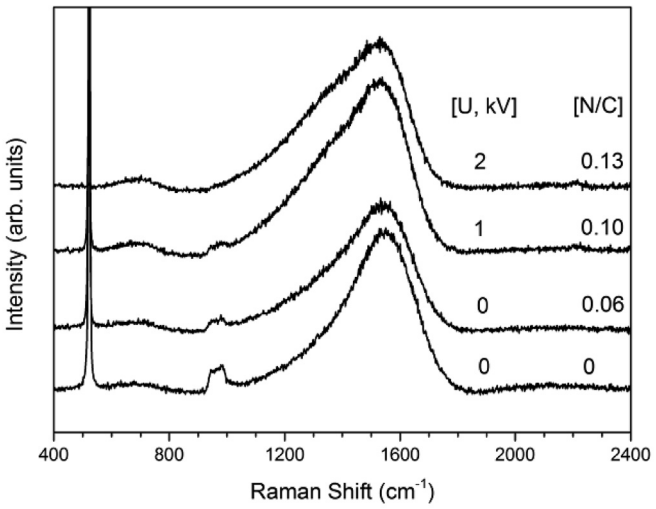

Fig. 5. Raman spectra of coatings obtained at different gas ion source voltages and having different nitrogen-carbon (N/C) ratios. The lower spectrum is for the coating obtained without nitrogen flood into the chamber.

with the sp^2 and sp^3 bonds.

To study the evolution of the sp^2 phase of the a-C:N coatings with increasing discharge voltage of the gas ion source and nitrogen concentration, Raman spectra were recorded (Fig. 5). The peaks in the spectra at 520 and 960 cm^{-1} correspond to the 1 s t and 2nd order lines of the silicon substrates. An increase in the discharge voltage of the ion source resulted in a decrease in the silicon line intensities and they vanished at U = 2 kV, which points to a reduction in the optical transparency of a-C:N.

The key features of the Raman spectrum obtained for the ta-C coatings (without N) in the visible region are the G and D peaks. The G peak is due to vibrations of any pairs of carbon atoms with the sp^2 hybridization and lies in the region 1500 - 1630 cm^{-1}. The D peak in the vicinity of 1360 cm^{-1} for graphite is associated with disordering. On the contrary, for amorphous carbon it points to the ordering process. Because of the similarity of the vibrational frequencies of the CC, CN, and NN bonds, difficulties are encountered in the interpretation of the Raman spectra of the ta-CN coatings. As shown in Ref. [15], Raman spectra of ta-C:N coatings can be analyzed from the point of view of the amorphous carbon model by decomposing into G and D peaks, without using additional peaks attributed to the CN and NN modes. Of greatest interest is the position of the maximum of the G peak and its full width at half-maximum (FWHM) and also the ratio between the intensities of the D and G peaks I(D)/I(G).

To obtain information on the positions of the G and D peaks, we approximated the experimental Raman spectra in the 1000-2000 cm^{-1} region with two Gaussian curves. The results are given in Table 1. It follows from the data presented in Table 1 that, as the discharge voltage of the ion source and the N/C ratio increase, the G peak shifts slightly towards lower wave numbers, the Full Width at Half Maximum (FWHM) decreases, and the ratio between the D and G peak intensities I(D)/I(G) increases. Such changes indicate that clustering of atoms having the sp^2 hybridization with the formation of sufficiently ordered structures occurs. They may also point to a general increase in the number of bonds with the sp^2 hybridization [15]. Thus, an increase in the discharge voltage of the gas ion source leads to increases in the nitrogen concentration in the amorphous carbon matrix and the number of atomic bonds with the sp^2 hybridization, which stimulates the sp^2 cluster formation.

For CN groups with sp^1-hybridization, a peak in the 2200 cm^{-1} region. This peak is absent at the spectra of the coatings obtained at U = 0 kV and is poorly distinguishable in the spectra of the coatings obtained at U = 1 and 2 kV (Fig. 4). The ratio between the intensities of the CN and G peaks I(CN)/I(G) is < 0.01.

Fig. 6a shows depth profile of the a-C thin films with a "delta-layer" of a-C:N. The relatively low concentration of around 10^{20}atoms/cm^3 for all elements forming residual atmosphere like H, O, and N in this film is observed. The thickness of the a-C:N layer was estimated as 75 nm by the Full Width at Half Maximum (FWHM). Fig. 6b shows the nitrogen distribution in the original sample and in the sample annealed at 1000 °C during 40 min. We conclude the absence of nitrogen diffusion under these conditions.

An important role in the efficient use of coatings in micromechanics, MEMS systems, and medical implants is played by the coating surface. Fig. 7 and Table 2 present results of analysis of AFM images of the surface relief of the a-C:N coatings obtained at different ion source voltages. It is evident that the roughness (Sq, Sa) of the 100 nm thick coatings is 4–6 times higher than the initial roughness of the sitall substrate. The coatings obtained at U = 0 kV are characterized by the lowest values of S10z, Sq, Sa, Sdr, Sds, and the height distribution density function A(z) has two peaks around 5.5 and 12 nm. An increase in U to 1 kV leads to the formation of a more developed surface relief, all the parameters given in Table 2 grow and reach their maximum values (except Sds). The A(z) function is a wide peak with a maximum in the vicinity of 15 nm. A further increase in U to 2 kV results in a slight decrease in the surface roughness parameters S10z, Sq, Sa, and Sdr. In this case, the density of the summits (Sds) is the highest, and their lateral dimension (d) is minimal. The A(z) function narrows, and the maximum shifts towards lower heights.

Electrical properties of the a-C:N coating surface are presented in Fig. 8 as functions of the current distribution density A (Ipr) over the surface. It can be seen that the coatings have an inhomogeneous distribution of electrical conductivity over the surface. A change in the discharge voltage of the ion source has an appreciable effect on the A (Ipr) function. The highest surface conductivity is displayed by the coating obtained at U = 1 kV, which agrees well with the resistivity measurements (Fig. 3).

The density, Young's modulus, and internal stresses of the a-C coatings without nitrogen and of the a-C:N coatings obtained at different voltages of the ion source are summarized in Table 3. The presence of nitrogen in the coating leads to decreasing density, Young's modulus, and also internal stresses. It is worth noting that the internal stresses in the ta-C coating can be as high as 10–12 GPa [4,8,13].

Table 1
Parameters of Raman spectra.

Sample		G-peak position (cm^{-1})	G-peak FWHM (cm^{-1})	I(D)/I(G)
a-C (free N)		1565	211	0.45
a-C:N	0 (kV)	1560	204	0.61
	1 (kV)	1557	184	0.88
	2 (kV)	1556	179	1.01

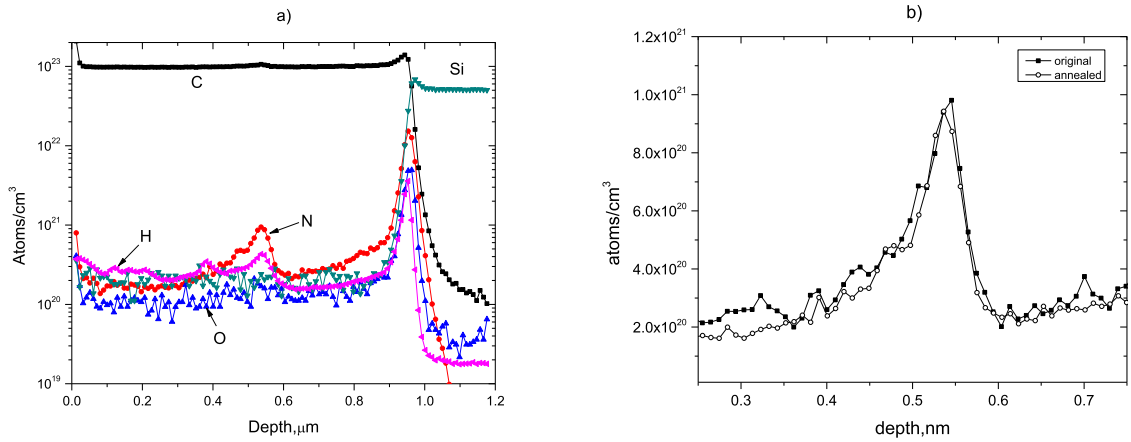

Fig. 6. SIMS depth profile of the N delta-doped a-C thin film (a); and the depth distribution of nitrogen in the original film, and in the same sample annealed at 1000 °C during 40 min (b).

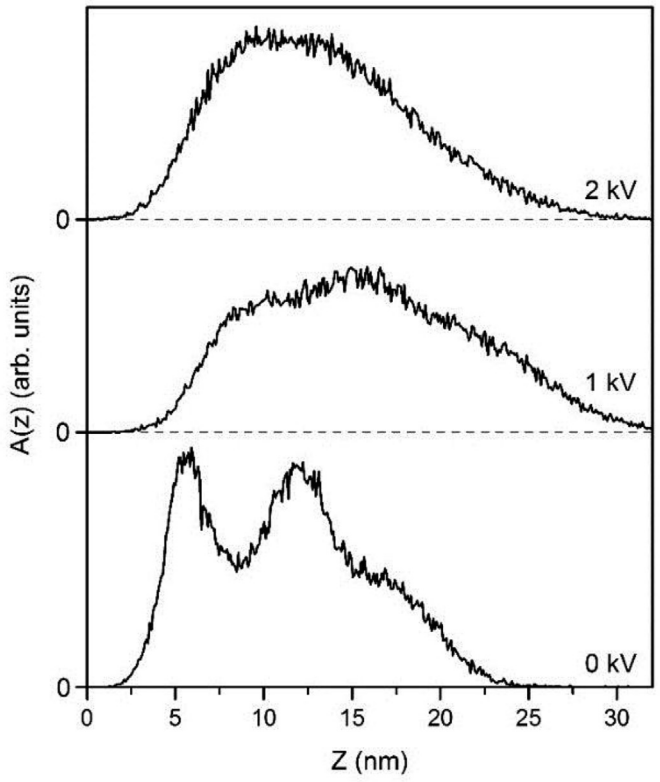

Fig. 7. Height distribution density functions of the relief A(z) of the a-C:N coatings formed at gas ion source voltages of 0, 1, and 2 kV.

4. Discussion

It is a widespread practice in magnetron sputter deposition and vacuum Arc deposition to apply a voltage offset of about −50 V ÷ −100 V to the substrate to accelerate plasma ions and bombard a growing film. Such an ion treatment does not result in sputtering of the growing film due to a low sputter rate for such an ion energy. It produces films with a higher density. In our experiments nitrogen ions with energies from 100eV to 2 keV were used to bombard the growing ta-C:N films. The ions with such energies penetrate to appreciably larger depths (up to 35 A for an 1 keV energy, as TRIM predicts [16]), and the ion sputtering effect for the deposited material is remarkable. So, let us dwell on the ion implantation and the ion sputtering effects.

After Sigmund [17], two different regimes in ion-solid interactions are considered: formation of linear cascades in a solid (LC) by primary ions, and formation of thermal spikes (TS), or non-linear regime. In the case of the LC regime only a small fraction of atoms in the cascade volume obtains enough energy to leave its lattice position (recoil atoms). The LC regime is used for primary ion energies from 5 keV to 25 keV. In the TS regime an essential part of the atoms (if not all) are in motion during the lifetime of the spike, typically for picoseconds. The TS regime is used, as a rule, for the heavy or cluster ion irradiation with the ion energy higher than 25 keV. The instantaneous temperature in such a cascade can reach thousands of degrees in K and exceeds the melting temperature of the target [18]. This can result in melting of the cascade area (melting pool formation) and its quick quenching with the formation of nano-clusters (or nano-crystals) embedded in an amorphous (or polycrystalline) matrix. This effect was observed experimentally, for example, for the Ti oxide [19] and Zr oxide [20] films deposited by the vacuum Arc method accompanied by an ion irradiation. Marks [21,22] considered theoretically the thermal spike formation in ta-C under a sub-keV ion irradiation. According to his estimates, the lifetime of TSs for ta:Si was about 0.1 ps and the TS radii were from 6 A to 12 A for the primary ion energy from 40eV to 400eV [21]. It was supposed that there was a strong temperature gradient inside such a cascade. Among others, Marks mentioned a nearly linear increase in the quenching time of the TSs with growing primary ion energy. At the same time, the increase in the quenching time correlates strongly with a decrease in the sp3 fraction in ta-C films [22]. A good correlation between Marks's calculations and the experimental results and simulations published by other authors for a-C and ta-C was demonstrated [21,22].

In our previous study [23] we considered the thermal spike formation under a low-energy (<5 keV) ion irradiation of relatively dense materials as well. The ion penetration depth Rp decreased proportionally to the square root of the primary ion energy ~ $Eo^{1/2}$ [24], but the volume of the cascade generated by the ions was proportional to ~$(Rp)^3$or to ~ $Eo^{3/2}$ in this case. Thus, the primary ion energy (Eo) released per unit volume in the cascade, or "the power" of the cascade, was proportional to ~ $Eo^{-1/2}$. This means that a decrease of the primary ion energy from a few keV to sub-keV resulted in an increase in the cascade power, or cascade instantaneous temperature [18], and vice versa. If the primary ion was not heavy or the target was not dense enough, we suggested a special "mixed regime": due to a statistical character of the ion-

Table 2
Surface parameters: S10z – ten point height of the surface; Sq – root mean square height of the scale-limited surface; Sa – arithmetical mean height of the scale-limited surface; Sdr –developed interfacial area ratio of the scale-limited surface; Sds – density of summits of the surface; d – average lateral diameter of summits of the surface.

Sample		S10z (nm)	Sq (nm)	Sa (nm)	Sdr (%)	Sds (1/μm^2)	d (nm)
Sitall substrate		4.1	1.0	0.8	–	–	–
a-C:N	0 (kV)	23.1	4.2	3.5	2.6	214	51.8
	1 (kV)	35.1	5.9	4.9	5.4	225	52.2
	2 (kV)	32.9	5.1	4.2	3.9	306	42.7

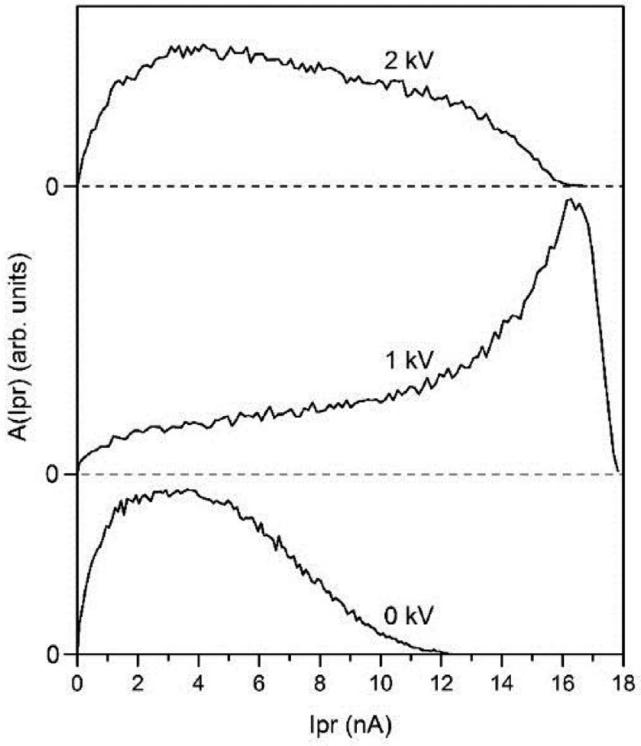

Fig. 8. Current distribution density functions A (Ipr) over surface of a-C:N coatings formed at gas ion source voltages of 0, 1, and 2 kV.

solid interaction a part of the cascades generated by primary ions was linear, but another part corresponded to TSs [23]. We suppose that nanocrystals of TiO and ZrO embedded in an amorphous target were obtained in the studies mentioned above in such a mixed regime [19,20].

By considering the estimates of Marks [21,22] and our "mixing regime" [23], we can explain the experimental data obtained in this study. Indeed, a very low ion irradiation (<100eV) during the ta-C deposition produces dense films with an internal stress and a high sp3 fraction. When the energy of irradiating nitrogen ions increases (>300eV), the cascade volume increases, and the quenching time of the thermal spikes increases too. This results in a decrease of the sp3 fraction. The increase of the D peak in the Raman spectrum (see Fig. 5) corresponds to the sp2 clustering, as demonstrated in Ref. [15]. The sp2 clustering growth was observed in our EELS spectra (Fig. 4). We believe that for such an experimental regime (300eV-2keV) the "mixed regime" with the formation of LCs together with TSs should be considered. However, we would like to consider another effect observed in ion irradiated targets for LCs. It is known that ion irradiation results in formation of point defects (vacancies) and adatoms. For some materials different mobilities of adatoms and vacancies were observed. This gave rise to the accumulation of vacancies in the target during the ion irradiation [25]. The formation of point vacancies in the nitrogen ion irradiated a-C:N films caused a decrease in its internal stress and density, and stimulate diffusion of nitrogen in growing film. The last explain the increase in the nitrogen concentration in our films.

It was mentioned in the literature that the growths in the sp2 fraction and nitrogen concentration lead to a decrease in the optical band gaps of a-C and ta-C films [3–5]. This correlates with the decrease in the resistivity of our a-C:N films.

The annealing experiment realized with the nitrogen "delta-doped" sample (Fig. 6) leads to another important conclusion. We did not observe any modification in the N depth distribution at 1000 °C, which means that nitrogen atoms formed strong chemical bonds with carbon atoms.

Ion irradiation produces, among other things, surface patterning, i.e., the formation of regular surface structures, such as nano-dots, nano-waves, etc. In our experiments the sputter rate for ta-C:N was lower than its deposition rate. This means that the models existing for surface patterning are not applicable. Thus, now we can only state that an increase in the surface roughness occurred due to the ion irradiation of the growing film. General conclusions can be made only when more experimental evidence is obtained.

5. Conclusion

It has been found that an increase in the intensity of nitrogen ion irradiation of an a-C:N coating during its formation from a pulsed carbon plasma flux under a constant nitrogen pressure in the chamber leads to an increase in the nitrogen content in the coating and clustering of atoms with sp^2 bonds, decreases in the electrical resistivity, density, modulus of elasticity, and internal stresses and a change in the morphology of the surface. The results obtained in our studies can be used for fabrication of conductive coatings with low internal stresses for micromechanics (MEMS), and, in particular, for improving the performance characteristics of silicon microprobes of scanning probe microscopes used in contact current-

Table 3
Density, Young's modulus, internal stresses.

Sample		Density (g/cm^3)	Young's modulus (GPa)	Internal stresses (GPa)
a-C (free N)		2.79 ± 0.13	340 ± 23	6.27 ± 0.25
a-C:N	0 (kV)	2.63 ± 0.15	254 ± 12	5.79 ± 0.22
	1 (kV)	2.52 ± 0.16	171 ± 7	3.14 ± 0.21
	2 (kV)	2.31 ± 0.19	146 ± 7	2.72 ± 0.18

conducting scanning techniques and current nanolithography. Tests of an experimental batch of silicon cantilevers coated by a-C:N films demonstrated a higher resource. It looks promising as production of ultrathin films with different resistivity using this method. Also, we found the absence of nitrogen diffusion for the temperature up to 1000 °C in a-C film grown by the vacuum arc deposition method.

Acknowledgments

The studies employed the equipment of the Joint Research Centre of "Diagnosis of the structure and properties of nanomaterials" in Belgorod State University supported by the Russian Foundation for Basic Research and the Belgorod Region Government in the framework of project No.15-48-03072. The authors from CINVESTAV thank the Conacyt (Mexico) for the partial financial support of this study, grant N 254903.

References

[1] E. Peiner, A. Tibrewala, R. Bandorf, H. Lüthje, L. Doering, W. Limmer, Diamond-like carbon for MEMS, J. Micromech. Microeng. 17 (2007) 83–90.
[2] G. Dearnaley, J.H. Arps, Biomedical applications of diamond-like carbon (DLC) coatings: a review, Surf. Coating. Technol. 200 (2005) 2518–2524.
[3] V.S. Veerasamy, J. Yuan, G.A.J. Amaratunga, W.I. Milne, K.W.R. Gilkes, M. Weiler, L.M. Brown, Nitrogen doping of highly tetrahedral amorphous carbon, Phys. Rev. B 48 (24) (1993) 17954–17959.
[4] L.K. Cheah, X. Shi, J.R. Shi, E.J. Liu, S.R.P. Silva, Properties of nitrogen doped tetrahedral amorphous carbon films prepared by filtered cathodic vacuum arc technique, J. Non-Cryst. Solids 242 (1998) 40–48.
[5] A.Ya Kolpakov, I.V. Sudzhanskaya, M.E. Galkina, I.Yu Goncharov, A.I. Poplavskii, S.S. Manokhin, Nanometer-sized carbon coatings on a silicon wafer: the effect that nitrogen doping level has on specific conductivity and morphology, Nanotechnologies in Russia 6 (2011) 185.
[6] Q. Wang, J. Jiang, An overview on structure and field emission properties of carbon nitride films, Journal of Nanomaterials (2014), 203837.
[7] A.Ya Kolpakov, A.I. Poplavsky, M.E. Galkina, I.V. Sudzhanskaya, I.Yu Goncharov, O.A. Druchinina, N.V. Strigunov, V.A. Kharchenko, O.Yu Merchansky, Properties of nanosized carbon coatings doped with nitrogen, tungsten, and aluminium and obtained by pulse vacuum arc method, Nanotechnologies in Russia 5 (3) (2010) 160–164.
[8] X.W. Zhang, N. Ke, W.Y. Cheung, S.P. Wong, Synthesis and structure of nitrogenated tetrahedral amorphous carbon thin films prepared by a pulsed filtered vacuum arc deposition, Diam. Relat. Mater. 12 (2003) 1–7.
[9] Y.H. Cheng, B.K. Tay, S.P. Lau, X.L. Qiao, J.G. Chen, Z.H. Sun, C.S. Xie, Micro-mechanical properties of carbon nitride films deposited by radio-frequency-assisted filtered cathodic vacuum arc, Appl. Phys. a 75 (2002) 375–380.
[10] A.I. Maslov, G.K. Dmitriev, YuD. Chistyakov, Impulsny istochnik uglerodnoy plasmy dlya tekcnologicheskih zeley, Pribory i tekhnika experimenta 3 (1985) 146–149 (in Russian).
[11] A.Ya Kolpakov, V.N. Inkin, and S.I. Ukhanov, RF patent No. 2240376 C1 (2004).
[12] K.V. Gogolinsky, N.A. Lvova, A.S. Useinov, Primenenie scaniruyushchih microscopov i nanotverdomerov dlya izucheniya mechanicheskich svoistv tverdych materialov, Zavodskaya laboratoriya 73 (6) (2007) 28–36 (in Russian).
[13] A.Ya Kolpakov, A.I. Poplavsky, M.E. Galkina, I.V. Sudzhanskaya, O.Yu Merchansky, Vliyanie ugla naklona plasmennogo potoka ugleroda k podlozhke I posleduyushego otzhiga na vnutrennie napryazheniya i structuru uglerodnykh nanorazmernykh pokryty, poluchennykh impulsnym vacuumno-dugovym methodom, Uprochnyayushie tehnologii I pokrytya 4 (2012) 40–45 (in Russian).
[14] A.C. Ferrari, A. Libassi, B.K. Tanner, V. Stolojan, J. Yuan, L.M. Brown, S.E. Rodil, B. Kleinsorge, J. Robertson, Density, sp3 fraction, and cross-sectional structure of amorphous carbon films determined by x-ray reflectivity and electron energy-loss spectroscopy, Phys. Rev. B 62 (2000) 11089–11102.
[15] A.C. Ferrari, S.E. Rodil, J. Robertson, Interpretation of infrared and Raman spectra of amorphous carbon nitrides, Phys. Rev. B 67 (2003), 155306–1–20.
[16] http://www.srim.org.
[17] P. Sigmund, Sputtering by ion bombardment: theoretical concepts, in: R. Behrisch (Ed.), Sputtering by Particle Bombardment ISpringer- Verlag, Berlin, 1981, p. 18.
[18] Yu Kudriavtsev, R. Asomoza, Collision cascade temperature, Nucl. Instrum. Meth. Phys. Res. B 266 (2008) 3540–3544.
[19] A. Bendavid, P.J. Martin, E.W. Preston, The effect of pulsed direct current substrate bias on the properties of titanium dioxide thin films deposited by filtered cathodic vacuum arc deposition, Thin Solid Films 517 (2008) 494–499.
[20] P.J. Martin, A. Bendavid, Properties of zirconium oxide films prepared by filtered cathodic vacuum arc deposition and pulsed DC substrate bias, Thin Solid Films 518 (2010) 5078–5082.
[21] N.A. Marks, Evidence for subpicosecond thermal spikes in the formation of tetrahedral amorphous carbon, Phys. Rev. B 56 (N5) (1997) 2441–2446.
[22] N.A. Marks, D.R. McKenzie, B.A. Pailthorpe, M. Bernasconi, M. Parrinello, Phys. Rev. B 54 (1996) 9703.
[23] A. Hernández, Yu Kudriavtsev, Bim+ ion beam patterning of germanium surfaces at different temperatures and ion Fluence, J. Vac. Sci. Technol. B 34 (6) (2016), 061805–1.
[24] H. Gnaser, Low-energy ion irradiation of solid surfaces, in: G. Hohler (Ed.), Springer Tracts in Modern Physics, vol. 146, Springer- Verlag, Berlin, 1999, p. 13.
[25] L. Bischoff, K.H. Heinig, B. Schmidt, S. Facsko, W. Pilz, Nucl. Instrum. Methods B 272 (2012) 198.